https://doi.org/10.5194/egusphere-2026-3927
Preprint. Discussion started: 23 July 2026


# The impact of climate extremes on northern and southern hemisphere seasonal ecosystem productivity over four decades to 2018

Andrew P. Scafaro[1] & Owen K. Atkin[1]

[1]Division of Plant Sciences, Research School of Biology, The Australian National University, Canberra 2601, Australia

**Correspondence:** Andrew P. Scafaro, Division of Plant Sciences, Research School of Biology, The Australian National University, Canberra 2601, Australia. Phone: +61261259580, Email: andrew.scafaro@anu.edu.au

**Abstract**

Climate extremes affect ecosystem performance across the globe, including net seasonal productivity (NSP), the difference between land surface carbon uptake in summer and release in winter. In this study we correlated estimates of NSP, obtained from atmospheric carbon (C) observations, with curated climate extreme indices that span from 1977 to 2018, split between the Northern (NH) and Southern hemispheres (SH). In the NH, wet climate extremes correlated with an increase in summer uptake of C, and hot climate extremes were correlated with reduced winter release of C. Together, hotter and wetter climate extremes in the NH correlated with increased NSP, a finding that supports a beneficial effect of warming climates in high latitude seasonal NH forests, where cold temperatures typically limit ecosystem productivity. In the SH, all 10 hot climate extremes examined correlated negatively with summer C uptake, and NSP in the SH was negatively correlated with hot extremes but positively correlated with wet and cold extremes. The results indicate that seasonality in the SH, which is predominately located in warm tropical and subtropical forests, seem to be more deleteriously impact by heat than the NH, presumably due to the ambient temperature of SH forests being already close to biological heat thresholds such as photosynthetic heat stability. Increases in the Southern Oscillation Index (SOI) in the NH was associated with wetter and hotter climates that drove down winter C loss and led to increases in NSP. In the SH an increase in the SOI was associated with wetter climates that correlated with increased summer C uptake and NSP. The findings highlight the contrast between NH and SH seasonal C flux responses to climate extremes, and

https://doi.org/10.5194/egusphere-2026-3927
Preprint. Discussion started: 23 July 2026


the importance of climate drivers of temperature and rainfall extremes in determining global ecosystem performance.

## 1 Introduction

Attributing the seasonal fluctuation in atmospheric carbon (C) concentrations to the terrestrial biosphere is well established, particularly for the Northern hemisphere (NH) and at higher latitudes (Graven et al., 2013; Forkel et al., 2016; Liu et al., 2024b). Fossil fuel use can vary seasonally, with as much as 5% more C released from fossil fuel burning in the NH winter than summer (Rotty, 1987). However, the seasonal cycle in anthropogenic C release is no more than 10% of the total seasonal atmospheric C cycle (Levin et al., 2003), with much of the seasonal cycle being driven by C exchange by plants and soils. Seasonal uptake in atmospheric C, and an increase in atmospheric $\delta^{13}C$ (due to $^{12}CO_2$ being fixed preferentially by Rubisco), directly link seasonal photosynthetic C uptake and atmospheric C concentrations (Von Caemmerer, 2020). Moreover, increases in seasonal ecosystem productivity from atmospheric $CO_2$ records and through global vegetation models closely align (Graven et al., 2013; Haverd et al., 2020; Ruehr et al., 2023; Zhu et al., 2016). With seasonal fluctuations in the atmospheric C cycle reflecting photosynthetic and respiratory flux, studies have used the atmospheric C data to infer patterns of change in seasonal ecosystem productivity (Forkel et al., 2016; Graven et al., 2013; Liu et al., 2024b).

Increases in the amplitude of the seasonal fluctuation in atmospheric C and net ecosystem productivity over recent decades have been linked to increasing seasonal productivity due to $CO_2$ fertilisation of photosynthesis, with that effect being stronger than negative influences on ecosystem productivity such as climate extremes and land clearing (Ruehr et al., 2023; Zhu et al., 2016). Importantly, the increase in amplitude of seasonal C is stronger the more north in latitude observations are made, suggesting that the $CO_2$ fertilisation effect is primarily occurring in boreal and temperate forests across northern land masses (Dunn et al., 2020).

A key area that needs to be addressed is understanding how greenhouse-gas induced increases in climate extremes (historically uncommon hot, cold, wet, and dry weather events) are influencing global patterns in seasonal productivity and associated seasonal changes in atmospheric C. Climate extreme indices derived from weather records can provide clear indicators of erratic changes in weather systems due to global warming. One such set of indices is held within the HadEX3 global climate extreme database (Dunn et al., 2020). Given that

https://doi.org/10.5194/egusphere-2026-3927
Preprint. Discussion started: 23 July 2026


there is climate extreme data that can be paired with seasonal ecosystem C exchange data, the opportunity exists to determine which climate extreme events have had an impact on seasonal changes in atmospheric C and associated patterns in ecosystem performance. An important driver of climate is the Southern Oscillation Index (SOI). The SOI captures differences in eastern and western equatorial Pacific Ocean sea-level pressures and temperatures that drive El Niño (wet eastern Pacific – low SOI) and El Niña (wet western Pacific – high SOI) (Rasmusson and Wallace, 1983). SOI has the potential to influence climate extremes, with knock-on effects on ecosystem productivity, atmospheric C and the global climate system.

While the NH is thoroughly studied in terms of its seasonal biosphere C exchange, the southern hemisphere (SH) has not been explored in a similar way, understandable as the SH has less of the seasonal forests found in the NH (seasonal atmospheric $CO_2$ fluctuations is much less evident in the SH - Fig. 1). Another difference between the NH and SH is that, unlike the NH, most of SH seasonality occurs in the lower < 25° latitudes, where most of the SH land vegetation resides. Despite reduced seasonality in the SH (Liu et al., 2024b), it is important to understand how climate extremes are impacting the forests in the SH, as much of the world's vegetation resides in SH tropical rainforests.

In this study we investigate hemisphere-specific relationships between seasonal variations in atmospheric C and climate extremes. We correlate seasonal summer C uptake, winter release, and seasonal uptake minus release (net seasonal productivity - NSP) with climate extremes by matching mean yearly data between seasonal C exchange and climate extreme records. By combining yearly seasonal productivity with yearly climate extreme data and changes in SOI, our goal was to provide generalised hemisphere-scale insights into which extremes in climate are driving seasonal C uptake and release from ecosystems. We explore factors determining differences in the response of vegetation above and below the equator to climate change drivers. The findings point to increases in the availability of water driving greater seasonal productivity, and the widening of the daily temperature range (DTR) driving reduced seasonal summer C uptake, across both hemispheres. Importantly, we show that there are clear differences in the impact of climate extremes on vegetation that are hemisphere based, the most evident being the impact of hot extremes. While NH seasonal productivity has mostly benefitted from an increase in hot climate extremes, the opposite has occurred in the SH, emphasising the difference in forest seasonality between the hemispheres and the importance of understanding SH seasonality despite it being less pronounced than the NH.

https://doi.org/10.5194/egusphere-2026-3927
Preprint. Discussion started: 23 July 2026


## 2 Materials and Methods

### *2.1 Data acquisition*

Four datasets were used in this analysis: (1) Northern Hemisphere atmospheric $CO_2$ concentration records from Mauna Loa (MLO, 20°N), Hawaii (NOAA); (2) Southern Hemisphere atmospheric $CO_2$ concentration records for Kennaook/Cape Grim (CGO, 41°S), Tasmania, Australia (Australian Bureau of Meteorology; CSIRO Oceans & Atmosphere); (3) The HadEX3 climate extreme indices with reference period of 1961-1990 for the years 1977 to 2018 (Dunn et al., 2020); and (4), the southern oscillation index (SOI) recordings derived from sea-level atmospheric pressure differences between Tahiti and Dawin (Australian Bureau of Meteorology). All analysis was limited to the years 1977 to 2018 based on $CO_2$ concentration data for Kennaook/Cape Grim starting in 1977, and the HadEX3 climate extreme database being limited to 2018. The HadEX3 data can be accessed from the Climdex online repository (https://www.climdex.org/access/). The atmospheric $CO_2$ concentration and SOI datasets used are available from the websites of the named government agencies above. The mean 1977 to 2018 annual values spit by hemisphere, covering all data used to generate results (the atmospheric C exchange data, HADEX3 data, and SOI data) can be found at https://dx.doi.org/10.25911/cfej-9t96.

### *2.2 A segmented linear model analysis of seasonal atmospheric carbon exchange*

Mauna Loa and Kennaook/Cape Grim are two of the three Premier Global Baseline stations of the World Meteorological Organisation's Global Atmospheric Watch programme, making them ideal representatives of atmospheric C observations for the NH and SH, respectively. Kennaook/Cape Grim observatory data consisted of monthly observations starting in 1977 and Mauna Loa observatory data (although available on a weekly basis and beginning in 1974) was limited to 1977 and monthly data for consistent analysis between the two observation sites. $CO_2$ was converted from a concentration to a mass in petagrams of atmospheric carbon (Pg C) by multiplying by a factor of 2.12 Pg C per ppm of $CO_2$ for all subsequent analysis; all results are thus presented on a C mass basis. To de-trend the interannual increases in atmospheric C, a quadratic equation was fitted through least-squares regression to the mean yearly atmospheric C over the years for which data were analysed (Fig. S1). From this quadratic equation, predicted atmospheric C values ($C_p$) at each datapoint were used to obtain the baseline atmospheric C independent of the annual upward trends as follows:

https://doi.org/10.5194/egusphere-2026-3927
Preprint. Discussion started: 23 July 2026


$$Baseline\ C_{[t_n]} = C_{o[t_n]} - \left(C_{p[t_n]} - C_{p[t_1]}\right) \quad \text{Eq.1}$$

where $C_o[t_n]$ is the observed atmospheric C at any given observation point, $C_p[t_n]$ is the predicted atmospheric C at any given observation point, and $C_p[t_1]$ is the predicted atmospheric C at the baseline observation year of 1977. Thus, all influences on inter-annual shifts in atmospheric C - notably rises in anthropogenic C emissions - were not factored into our seasonal analysis. The annual sea-air C flux was also assumed to not influence the analysis, being less than 10% of the NH seasonal C cycle (Zhang et al., 2022), but may have had a greater influence on the much smaller SH seasonal atmospheric cycle.

A linear model framework with break-points determined through fitted piecewise terms in the regression model, as described by Muggeo (2003), was used to determine the peak and trough of each yearly seasonal fluctuation in atmospheric C, with the model providing estimates of atmospheric C at the peak and trough of each cycle. Firstly, the baseline atmospheric C data were subset by time of year so that the peak and trough of seasonal atmospheric C was separately analysed using the segmented linear model. For the NH, January to July observations captured the peak in atmospheric C (equivalent to the end of vegetative carbon release), and July to December for the trough of atmospheric C (equivalent to the end of vegetative carbon uptake). For the SH, January to July observations captured the trough in atmospheric C and June to December for the peak of atmospheric C. Linear models using the 'segmented' package in R (Muggeo, 2003; Muggeo et al., 2014) were able to fit a break-point at the seasonal peak and trough and linear regressions either side (Fig. S2). Seasonal uptake rate (Tg C $day^{-1}$) was derived from the slope of the linear regression between a peak and trough. Seasonal release rate was derived from the slope of the linear regression between a trough and peak. The seasonal uptake span (days) was derived from the number of days between a peak and trough, or between a tough and peak for release span. A seasonal uptake and release (Pg C) were derived from the seasonal uptake and release rates multiplied by the span of uptake and release days. Finally, net seasonal productivity was derived by subtracting the seasonal release from the seasonal uptake of C.

*2.3 Global climate extreme indices*

The HadEX3 global climate extreme index covers weather indices interpolated from annual and monthly observations from weather stations on a 1.875×1.25° grid derived from daily in situ weather station observations from the years 1950 to 2018 and referenced to the years 1961-

https://doi.org/10.5194/egusphere-2026-3927
Preprint. Discussion started: 23 July 2026


1990, as described by Dunn et al. (2020). We averaged indices for the entire NH and SH geographical regions by year from 1977-2018. The dataset is curated until 2018, limiting our analysis to that year. We categorised the indices into five climate categories: temperature range (one index), dry (one index), hot (10 indices), cold (five indices), wet (nine indices). The single temperature range index was the diurnal temperature range (DTR), which was the annual mean difference between daily max and min temperatures (°C). The single dry index was the consecutive dry days (CDD), which was the highest number of consecutive days when precipitation < 1 mm. The 10 hot indices were: TXx, the annual highest value of maximum daily temperature; TXn, the annual lowest value of the maximum daily temperature; TX90p, the percentage of days when maximum daily temperature is > 90$^{th}$ percentile; TNx, the annual highest value of daily minimum temperature; TNn, the minimum value of daily minimum temperature; TN90p, the percentage of days when maximum nighttime temperature > the 90th percentile; GSL, the annual growing season length; SU, the number of summer days when the daily maximum temperature was > 25°C; TR, the number of tropical nights when maximum nighttime temperature was > 20°C; and WSDI, the warm spell duration index - annual count of days with at least 6 consecutive days when maximum daily temperature was > 90th percentile. The five cold indices were: TN10p, the percentage of days when the daily minimum temperature was < the 10$^{th}$ percentile; TX10p, the percentage of days when the daily maximum temperature was < 10$^{th}$ percentile; CSDI, the cold spell duration index - annual count of days with at least 6 consecutive days when the daily minimum temperature was < the10th percentile; FD, the number of frost days with daily minimum temperature below 0°C; and ID, the number of icing days when the daily maximum temperature was < than 0°C. The nine wet indices were: R95p, the annual total PRCP when the daily precipitation amount was > 95$^{th}$ percentile; R99p, the annual total PRCP when the daily precipitation amount was > 99$^{th}$ percentile; Rx1day, the maximum 1-day precipitation; Rx5day, the maximum consecutive 5-day precipitation; R10mm, the annual count of days when precipitation was ≥ 10mm; R20mm, the annual count of days when precipitation was ≥ 10mm; CWD, the maximum length of a wet spell - daily precipitation amount ≥ than 1 mm; PRCPTOT, the annual total precipitation on wet days; and SDII, the simple precipitation intensity index. For a more detailed explication of how each indices was calculated, refer to Dunn et al. (2020). Note that categorisation of an indices as hot or cold was based on a positive association with the climate category. For instance, TXn and TNn although measuring the lowest value of the annual maximum and minimum daily temperature are classified as hot extreme indices because a higher TXn or TNn value indicates a hotter climate.

https://doi.org/10.5194/egusphere-2026-3927
Preprint. Discussion started: 23 July 2026


*2.4 Data analysis by year or SOI*

Data was analysed using base R programming language. Correlations between seasonal C exchange (seasonal uptake, seasonal release, and net seasonal productivity) and year, or between seasonal C exchange and SOI, were based on linear regression analysis of the mean value for each variable, segmented by year of observation. The yearly mean seasonal carbon exchange variables and SOI were further correlated with corresponding yearly means of extreme climate indices, and the presented correlation coefficients between the variables of interest are based on a Persons correlation matrix performed in Base R programming language.

## 3 Results

*3.1 Seasonal carbon exchange in the northern and southern hemisphere*

Yearly fluctuations in atmospheric C attributed to variations in vegetative C cycles were evident in both the NH and SH (for the years 1977-2018) when subtracting background anthropogenic rises in atmospheric C (Fig. 1a). Predictions of atmospheric C using the segmented linear model closely matched observations over all the years analysed, with a RMSE value of 0.37 Pg for the NH and 0.097 Pg for the SH and an $r^2$=0.99 for both (Fig. 1b). The model accuracy gives support to our seasonal uptake and release calculations that were based on the slopes and identified peak and trough positions of the segmented linear model.

There were weak and non-significant ($P > 0.05$) linear relationships in seasonal C exchange rates (Fig. 2a), C uptake and release spans (Fig. 2b), total seasonal C uptake and release (Fig. 2c), and NSP for both the NH and SH (Fig. 2d; Table S1). Taken together, the combination of (1) a faster seasonal uptake rate multiplied by a shorter uptake season, and (2) a slower seasonal release rate multiplied by a longer release season, led to almost matching total seasonal uptake and release of C each year in the NH. The resulting net seasonal productivity (NSP) in the NH was close to zero across the years 1977-2018 with an upward trend through time by 0.015 Pg C $yr^{-1}$ (Fig. 2d); while this upward trend was not significant, it equated to a 0.1% increase in NSP $yr^{-1}$ relative to the 15 Pg C of seasonal uptake in 1977. Interestingly, the SH seasonal uptake span was longer than the release span (Fig. 2b) and the seasonal C uptake rate was slower than the release rate (Fig. 2c), the reverse of the relationship between rates and seasonal span in the NH. As with the NH, SH differences in seasonal rates between uptake and release were largely counteracted by the span of the uptake and release season, leading to near zero NSP that was almost constant from the years 1977-2018, barely increasing by 0.001 Pg C $yr^{-1}$.

https://doi.org/10.5194/egusphere-2026-3927
Preprint. Discussion started: 23 July 2026


235

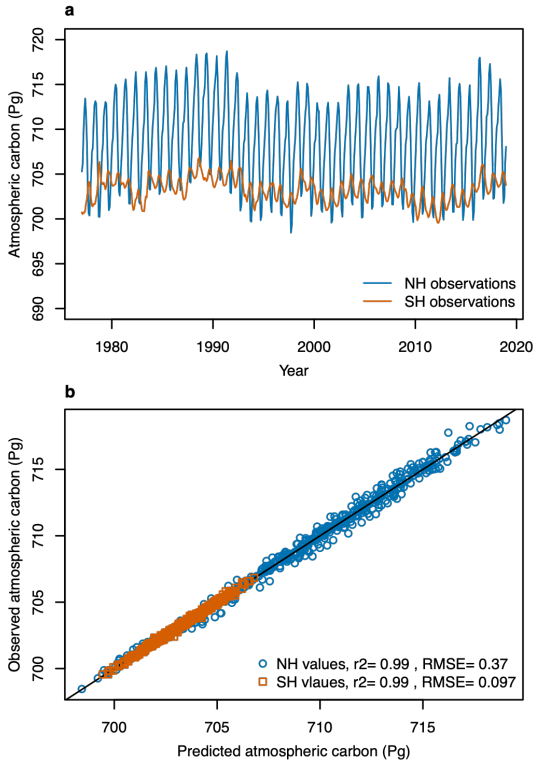


236

237 **Figure 1.** Atmospheric carbon (C) observed from Mauna Loa, Hawaii (NH) and Kennaook/Cape Grim, Tasmania
238 (SH), two of the three Premier Global Baseline stations of the World Meteorological Organisation's Global
239 Atmospheric Watch programme. (a) Observations were limited to the years 1977-2018 with the yearly upward
240 trend in emissions removed (refer to Eq.1 and Fig. S1). (b) Model analysis of observed atmospheric C compared
241 to predicted atmospheric C based on a segmented linear model of observed data to derive seasonal C uptake and
242 release. The $r^2$ and the Root Mean Square Error (RMSE) values of the modelled versus observed values are
243 presented on the graph.

244

https://doi.org/10.5194/egusphere-2026-3927
Preprint. Discussion started: 23 July 2026


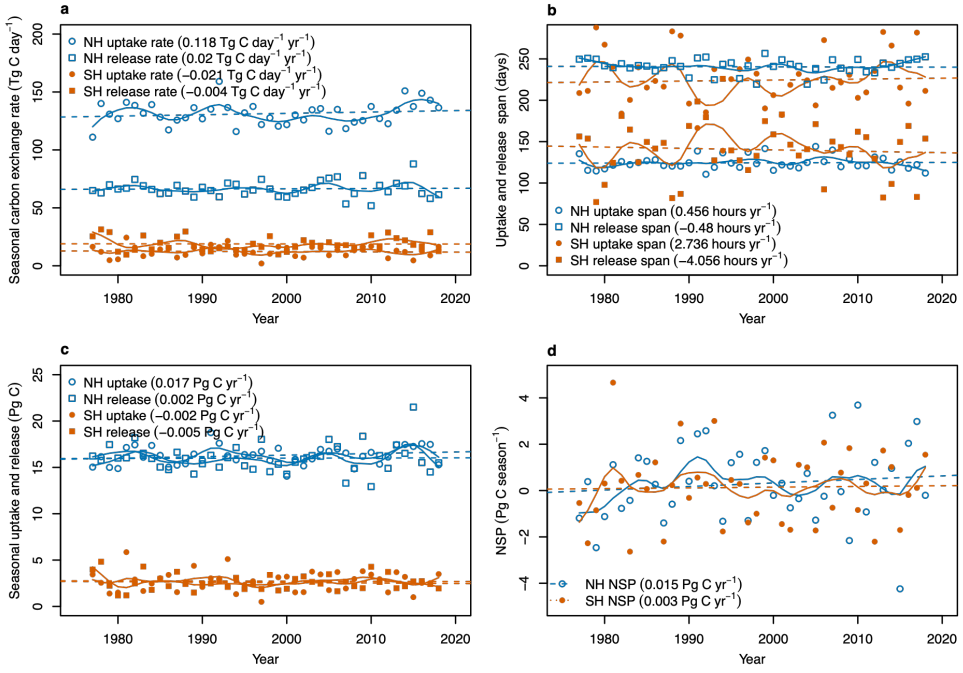


**Figure 2.** Seasonal ecosystem carbon exchange in the Northern (NH) and Southern hemisphere (SH) based on a segmented linear model that determined the peak and trough, and the rate of seasonal uptake and release of each yearly seasonal fluctuation in atmospheric carbon. (a), Seasonal C exchange rates based on the linear rate of decline or incline in atmospheric C between the peak and trough (uptake) or trough and peak (release) during the warmer and cooler months in each hemisphere. (b) The seasonal C uptake and release span based on the days between the peak and trough (uptake) or trough and peak (release) during the warmer and cooler months in each hemisphere. (c) The total seasonal C uptake and release based on the uptake and release rates in Panel a multiplied by the seasonal span presented in Panel b. (d), The Net Seasonal Productivity (NSP) based on subtracting seasonal uptake from seasonal release as presented in Panel c. Stright dashed lines represent the linear regression fits between seasonal C exchange variables and year with the slope coefficients of regression fits presented in parenthesis in the figure legends and more detailed regression statistics presented in Table S1. Curved lines represent a cubic smoothing spline fit.

### *3.2 Climate extreme correlations with time and seasonal carbon exchange*

When averaged by year, a range of indices of hot climate extremes exhibited strong positively correlations with chronological time from 1977 to the 2018 (Fig. 3). Stronger correlations were evident in the SH, where all 10 hot climate extreme indices were most positively correlated with progression of time. While the top three climate extremes positively correlated with year in the NH were also hot extremes (TN90p, WSDI, and TX90p), other hot climate extremes were negatively correlated with year in the NH (TR, SU, and TXn). The other clear difference

https://doi.org/10.5194/egusphere-2026-3927
Preprint. Discussion started: 23 July 2026


266 between the two hemispheres in climate extreme patterns with time was a positive correlation
267 between wet climate extremes and year in the NH, with all eight wet climate extremes
268 positively correlating with progression of year in the NH, and to a much greater extent than
269 wet climate extremes in the SH (Fig. 3).
270

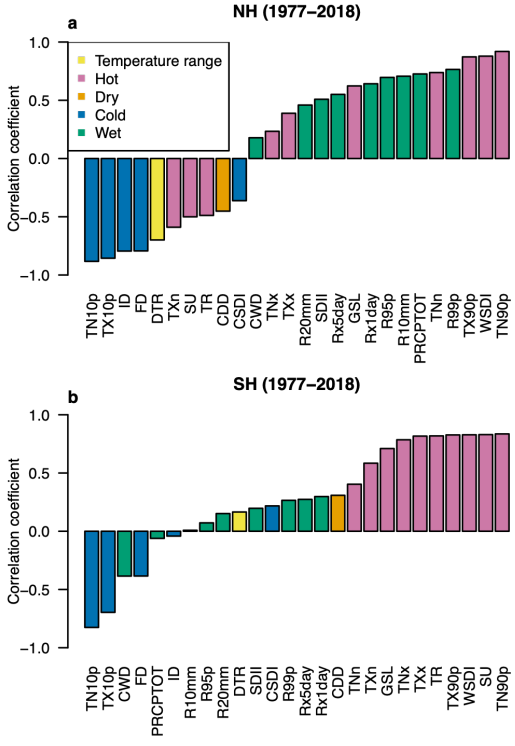

271

272 **Figure 3.** Pearson correlation matrix derived correlation coefficients for the relationships between the annual
273 mean values of each temperature extreme index and chronological time spanning the years 1977-2018 in the
274 northern hemisphere (a) and the southern hemisphere (b). The HadEX3 climate extreme indices are colour coded
275 by climate category as presented in the legend. Climate index acronyms are described in the Methods section of
276 this report, and are described in detail by Dunn et al. (2020).
277

278 Pearson correlation matrices further allowed for associations between annual mean
279 changes in seasonal C exchange (i.e. uptake, release, and NSP) and climate extremes among
280 the years 1977-2018 to be ascertained. In both the NH and SH, seasonal C uptake was to the
281 greatest extent positively correlated with wetter climate extremes (Fig. 4). Hot and cold climate
282 extremes had differing relationships with seasonal C uptake depending on the hemisphere (Fig.
283 4a,b). Hot climate extremes were often correlated with increased seasonal C uptake in the NH

https://doi.org/10.5194/egusphere-2026-3927
Preprint. Discussion started: 23 July 2026


(TN90p, WSDI, TX90p, GSL) but all hot extremes had a negative correlation with seasonal carbon uptake in the SH. Indeed, in the SH, eight of the nine climate extremes most negatively correlated with C seasonal uptake were heat related. All five cold climate extremes were negatively correlated with seasonal C uptake in the NH, while in the SH three of the five cold extremes (indices FD, TN10p, and TX10p) all correlated positively with seasonal carbon uptake. In both hemispheres, the climate extreme variable that had the strongest negative correlation with seasonal C uptake was Daily Temperature Range (DTR) (Fig. 4a,b).

There were distinct differences in climate extreme relationships with seasonal C release between the hemispheres (Fig. 4c,d). Most strikingly, hot climate extremes negatively correlated with seasonal C release in the NH, most notably TNx and TXx were the two hot indices that correlated most negatively with C release (Fig. 4c). However, many hot extremes were positively correlated with seasonal C release in the SH (most notably, TX90p and WSDI). In the NH, wet and hot climate extremes positively correlated with NSP (Fig. 4e), while in the SH, wet and cold climate extremes positively correlated with NSP and hot extremes corelated with reduced NSP (Fig. 4f).

*3.3 Seasonal carbon exchange and the southern oscillation index*

To determine if the southern oscillation index (SOI) impacted on seasonal C uptake or release over the past few decades for both the NH and SH, the mean yearly seasonal C exchange values were further compared to SOI values for the same years (Fig. 5). The SOI had a significant negative relationship with NH seasonal release, and a subtle non-significant negative relationship with NH uptake. In the SH, SOI had a positive and significant relationship with SH seasonal C uptake and non-significant relationship with SH release. The resulting impact of the SOI on overall NSP was a significant positive relationship in both hemispheres (Fig. 5b). The significant positive relationship between SOI and NSP in the NH can be attributed to the SOI being strongly correlated with wetter and hotter climate extremes in the NH (Fig. 5c), extremes that were shown to correlate with reduced NH seasonal release and increased NSP (Fig. 4 c,e). The significant positive relationship between SOI and NSP in the SH can be attributed to the SOI being strongly correlated with wetter climate extremes in the SH (Fig. 5d) and these extremes being positively correlated with seasonal uptake and NSP in the SH (Figs. 4b,f & 5d).

https://doi.org/10.5194/egusphere-2026-3927
Preprint. Discussion started: 23 July 2026


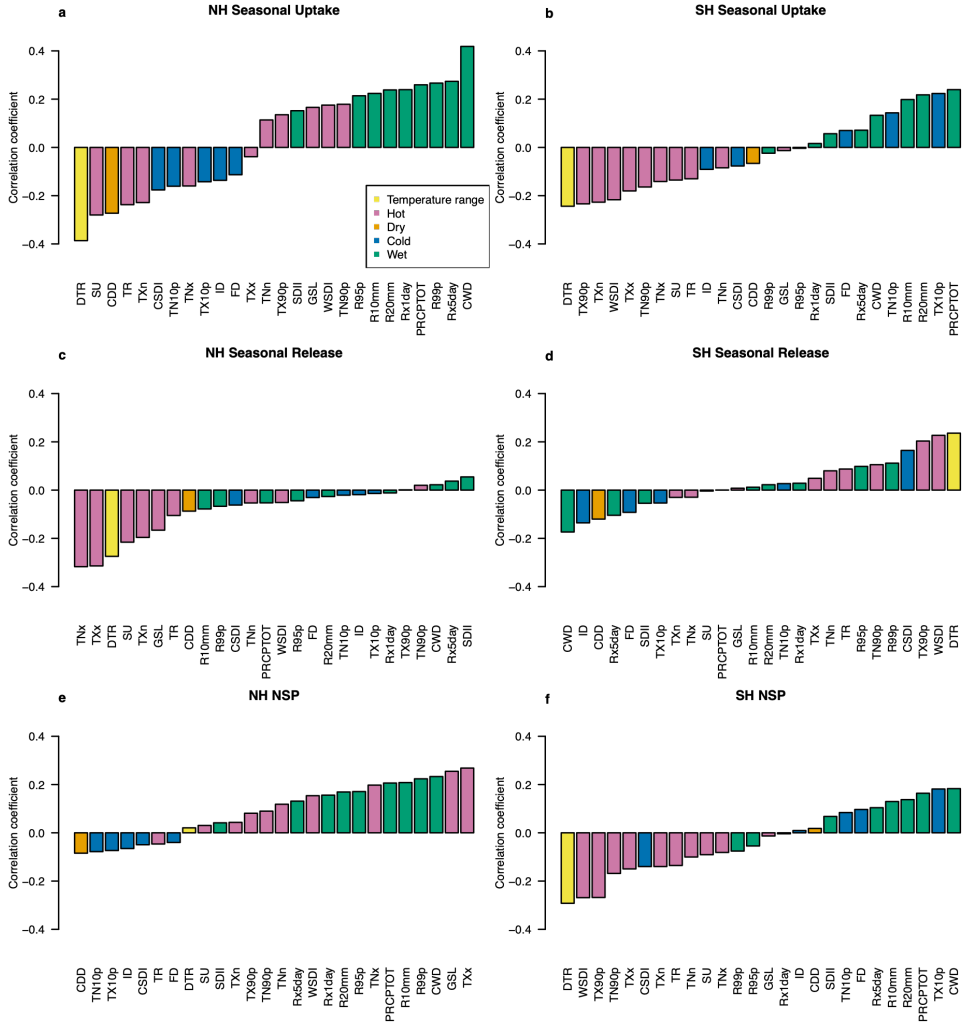


**Figure 4.** Pearson correlation matrix derived correlation coefficients for the relationships between the annual mean values of each temperature extreme index and annual mean seasonal C ecosystem exchange variables, for the northern (NH) and southern hemispheres (SH). (a,b), The relationships between seasonal C uptake (as presented in Fig. 2c) and climate extreme indices. (c,d), The relationships between seasonal C release (as presented in Fig. 2c) and climate extreme indices. (e,f), The relationships between net seasonal productivity (NSP) (as presented in Fig. 2d) and climate extreme indices. The HadEX3 climate extreme indices are colour coded by climate category as presented in the legend. Climate index acronyms are described in the methods section of this report, and are described in detail by Dunn et al. (2020).

https://doi.org/10.5194/egusphere-2026-3927
Preprint. Discussion started: 23 July 2026


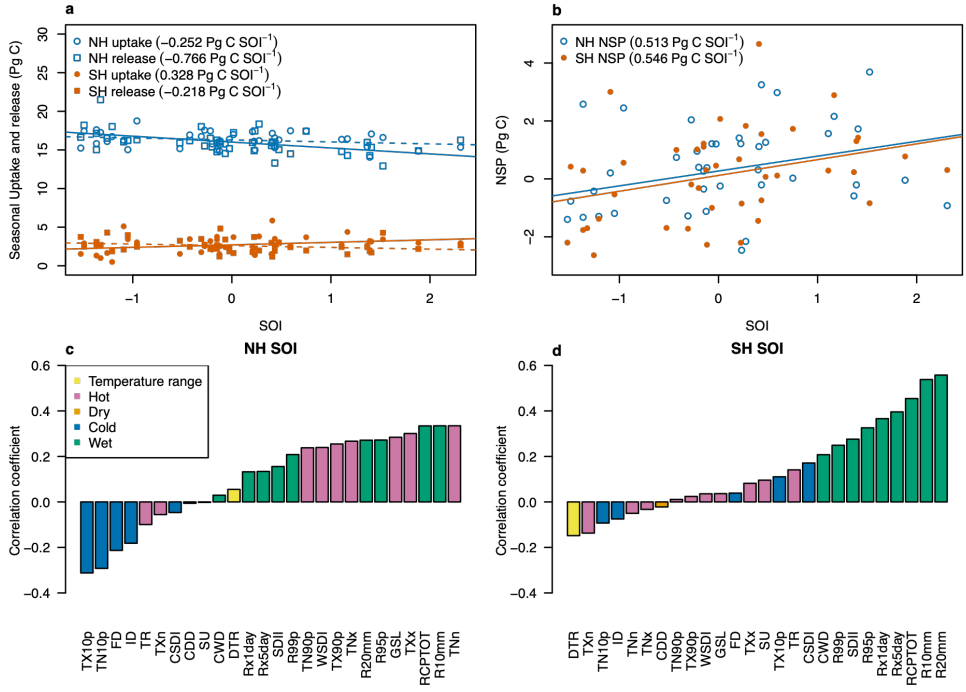


**Figure 5.** The relationships between seasonal C exchange variables and the Southern Oscillation Index (SOI) for the northern (NH) and southern hemispheres (SH). (a) The annual mean seasonal ecosystem uptake and release plotted against the annual SOI for the years. (b), The annual mean net seasonal productivity (NSP) plotted against the annual SOI. (c,d) Pearson correlation matrix derived correlation coefficients for the relationships between the annual mean values of each temperature extreme index and the annual mean southern hemisphere SOI for NH and SH, respectively. (a,b) Lines represent the linear regression fits between seasonal C exchange variables and SOI, with dashed lines representing no-significance ($p > 0.05$) and solid line representing significance ($P < 0.05$). The slope coefficients of regression fits are presented in parenthesis in the figure legends and more detailed regression statistics presented in Table S1.

## 4 Discussion

Ecosystem productivity has been rising steadily over past decades driven by atmospheric $CO_2$ fertilisation that has so far over-compensated for the negative impacts of climate extremes on photosynthetic performance (Ruehr et al., 2023). The impact of climate extremes on evergreen forests - particularly globally dominant tropical evergreen forests - will be the greatest contributor to carbon sequestration in plants (Pan et al., 2011). However, the positive and negative influences of climate extremes on seasonal C uptake, C release and resulting NSP, and differences between the NH and SH in seasonality responses to climate extremes is of urgent consideration. Indeed, shifts in seasonal productivity due to temperature dependence has

https://doi.org/10.5194/egusphere-2026-3927
Preprint. Discussion started: 23 July 2026


recently been identified as contributing most to $CO_2$ driven changes in global gross primary productivity, more so than changes in global mean annual temperature, mean annual precipitation, or aridity (Tang et al., 2025). Here, we identify that a rise in hot extremes and reduction in cold extremes benefits seasonal productivity in forests of the NH but are detrimental to SH seasonal productivity. This may have profound implications on the balance of seasonal vegetation and its distribution across the globe.

The NSP of the NH trended upwards at 0.1% NSP $yr^{-1}$ (Fig. 2). A similar weak and non-significant increasing trend of 0.076% $yr^{-1}$ was obtained from Mauna Loa observations analysed over a similar timeframes of 1970 to 2011 using amplitude of the seasonal C cycle (Forkel et al., 2016). However, others have reported a more substantial ~0.3% $yr^{-1}$ increase in seasonal amplitude over similar timeframes based on Mauna Loa observations (Cuntz et al., 2025; Graven et al., 2013), demonstrating variability in seasonal estimates of C uptake and release, likely due to the specifics of methodology and the years analysed. Observations based on vegetative indices from aeroplane surveys and satellite data, combined with biophysical models of photosynthesis, derive much higher increases in seasonal uptake for latitudes of > 40°N, ranging from 10 to 60% (or 0.1 to 0.8% $yr^{-1}$) over the years 1960-2010 (Haverd et al., 2020). There is, however, a positive relationship between seasonal productivity and NH latitude, attributable to more climate stimulation of boreal and tundra forests that are benefiting not only from atmospheric $CO_2$ fertilisation but also climate warming (Forkel et al., 2016; Haverd et al., 2020).

The atmospheric observations we present demonstrate seasonal C exchange differences that can be attributed to differences in the NH and SH biomes. In the NH, faster seasonal uptake rates were paired with shorter seasonal C uptake spans, reflecting cool environments with short but substantive warm season growth. By contrast, slower seasonal C uptake rates in the SH were paired with longer seasonal uptake spans, reflecting warm environments with limited seasonality but a longer growing season due to less distinct winter seasons in the SH forests (Fig. 2). This is consistent with the peak in C uptake by the land sink in the NH occurring at latitudes between 40 and 60°N (colder temperate forests), while land surface C uptake peaks at latitudes between 0 and 20°S (tropical and subtropical forests) in the SH (Haverd et al., 2020).

Hotter extremes are often associated with reduced plant performance (Margalef-Marrase et al., 2020; Teskey et al., 2015). This is evident in our SH analysis, with essentially all hot extreme indices correlating negatively with seasonal C uptake, positively with seasonal C release, and negatively with NSP (Fig. 4). This is despite the possibility of a small

https://doi.org/10.5194/egusphere-2026-3927
Preprint. Discussion started: 23 July 2026


confounding effect of hot extremes rising alongside $CO_2$ fertilisation, the latter, as previously stated, having a positive influence on plant productivity. Hot weather extremes can therefore be considered as one of the main drivers of loss of net seasonal C productivity by plants in the SH. Most of the vegetation in the SH is within the tropical and subtropical regions of central and southern parts of Africa, South America, southern part of Asia, and the north of Australia, regions where plant metabolism is not cold limited, but rather closer to the upper thermal limits of photosynthetic functionality. For example, a study of the tropical rainforests of the Amazon basin and the African Congo, showed that C uptake by the forests was negatively correlated with rising temperature, even more so than drier conditions (Hubau et al., 2020). Moreover, recent studies have reported that leaf temperatures in SH tropical forests often exceed their photosynthetic temperature optimum and may be reaching critical heat loads above photosynthetic biochemical stability that impact on survival (Doughty et al., 2023; Slot and Winter, 2017). The detrimental impact of hot climate extremes on NSP in the SH was not evident in the NH. Rather, warmer climate extremes were correlated with increased NSP in the NH. For example, the indices WSDI and TN90p that indicate spells of warm weather and mild nights during summer months were two of the climate extremes with strongest positive correlation to increase seasonal C uptake in the NH. The positive effect of hot climate extreme indices on NSP in the NH but not SH matches patterns of more climate resilience in northern latitude forests attributed to the positive influence of rising temperature and $CO_2$ fertilisation on biomass production in these high latitude NH forests (Forzieri et al., 2022).

The climate extremes indices with the greatest negative relationship with seasonal summer C uptake, for both hemispheres, was the diurnal temperature range (DTR). This suggests that a greater difference between the minimum and maximum daily temperature has a strong negative impact daily net C gain in summer months. One potential reason may be that a greater rise in diurnal air temperature would cause a rise in the atmospheric vapour pressure deficit (VPD) that can lead to stomata closure to limit accelerated leaf water loss, at a cost to photosynthetic C fixation, especially in afternoons as VPD rises (Grossiord et al., 2020; Liu et al., 2024a). Additionally, dynamic rises in temperature initiate kinase receptors that induce heat shock transcription factors and heat shock proteins for stabilisation of membrane lipids (Wang et al., 2026), all of which would presumably require energy and contribute to C loss. Of note, DTR is declining with time in the Northern hemisphere (Fig. 3a), likely driven by asymmetric warming in daily nighttime minimum relative to maximum temperatures, which is more pronounced in the NH (Davy et al., 2017). This yearly reduction in DTR is likely having a

https://doi.org/10.5194/egusphere-2026-3927
Preprint. Discussion started: 23 July 2026


positive influence on net C uptake in the NH considering the negative relationship between DTR and seasonal uptake.

Driven by a decline in NH seasonal release and an increase in SH seasonal uptake with increasing SOI, the SOI significantly correlate with positive changes in NSP in both hemispheres (Fig. 5). In the NH this positive correlation between SOI and NSP could be attributed to the SOI being associated with hotter climate extremes that were linked to reduced NH seasonal winter C release (Figs. 4c & 5c). In the SH the positive correlation between SOI and NSP could be attributed to much wetter climates with increased SOI driving increased SH seasonal summer C uptake and NSP (Figs. 4b,f & 5d). This is consistent with lower SOI (i.e. El Niño events) leading to drought, including in southern tropical rainforests, which severely reduces forest C uptake (Nath et al., 2024). As far back as the years 1997/1998, increases in tree mortality of 11 to 22% with an El Niño (i.e. low SOI) associated drought have been observed in the tropical forests of Borneo in Indonesia, just south of the equator (Slik, 2004). Of concern is a report that there may be an increase in the occurrence of intense El Niño SOI events associated with the human induced climate change (Cai et al., 2021), which will likely have a strong negative impact on seasonal productivity across the globe based the findings we present here.

## 5 Conclusions

In conclusion, ecosystems that seem to benefit the most from current changes in climate are seasonal cool temperate forests in the NH that are stimulated by wetter summers that increase C uptake, and hotter climate extremes that reduce winter C release. By contrast, hot climate extremes have reduced seasonal ecosystem performance in the SH through being negatively correlated with summer C uptake, most likely due to seasonality in the SH being concentrated in forests close to the equator that are already close to their photosynthetic temperature optimums. If these relationships between hot climate extremes and seasonal photosynthetic and respiratory C fluxes hold over the coming years, in essence, the NH may become greener and the SH less so. The extent to which seasonal productivity is detrimentally impacted upon by climate change may be most heavily dependent on the SOI, which is positively corelated with NSP across the hemispheres due to higher SOI (La Niña events) driving wetter climates in the SH and hotter and wetter climates in the NH. Whether these patterns hold as climate extremes become more intense over the coming decades and to what extent seasonal responses reflect general ecosystem performance to climate extremes needs to be further explored.

https://doi.org/10.5194/egusphere-2026-3927
Preprint. Discussion started: 23 July 2026


*Data availability.* All data used were accessed through publicly available sites: NOAA GML atmospheric $CO_2$ data was accessed at https://gml.noaa.gov. and Cape Grim atmospheric $CO_2$ data from https://capegrim.csiro.au. The SOI data from the Australian BOM at https://www.bom.gov.au/climate/enso/soi/. HadEX3 climate extreme data is available from the Climdex https://website www.climdex.org. Compiled annual mean values of all data split by hemisphere are located at the DOI: https://dx.doi.org/10.25911/cfej-9t96.

*Author contributions.* APS conceived and wrote the manuscript with revisions by OKA.

*Competing interests.* The authors declared that they have no conflict of interest.

*Acknowledgements.* We thank the agencies and institutions that have collected atmospheric $CO_2$ data and compiled climate extreme data used in this report. We thank the Australian Research Council (ARC) for support through Discovery Project grants (DP220101882, DP230103122, DP250104172).

**References**

Cai, W., Santoso, A., Collins, M., Dewitte, B., Karamperidou, C., Kug, J.-S., Lengaigne, M., McPhaden, M. J., Stuecker, M. F., Taschetto, A. S., Timmermann, A., Wu, L., Yeh, S.-W., Wang, G., Ng, B., Jia, F., Yang, Y., Ying, J., Zheng, X.-T., Bayr, T., Brown, J. R., Capotondi, A., Cobb, K. M., Gan, B., Geng, T., Ham, Y.-G., Jin, F.-F., Jo, H.-S., Li, X., Lin, X., McGregor, S., Park, J.-H., Stein, K., Yang, K., Zhang, L., and Zhong, W.: Changing El Niño–Southern Oscillation in a warming climate, Nature Reviews Earth & Environment, 2, 628-644, 10.1038/s43017-021-00199-z, 2021.

Cuntz, M., Smith, B., Canadell, J. G., Knauer, J., and Haverd, V.: Large and increasing biospheric productivity of northern ecosystems, Geophysical Research Letters, 52, e2025GL115983, https://doi.org/10.1029/2025GL115983, 2025.

Davy, R., Esau, I., Chernokulsky, A., Outten, S., and Zilitinkevich, S.: Diurnal asymmetry to the observed global warming, International Journal of Climatology, 37, 79-93, 10.1002/joc.4688, 2017.

Doughty, C. E., Keany, J. M., Wiebe, B. C., Rey-Sanchez, C., Carter, K. R., Middleby, K. B., Cheesman, A. W., Goulden, M. L., da Rocha, H. R., Miller, S. D., Malhi, Y., Fauset, S., Gloor, E., Slot, M., Oliveras Menor, I., Crous, K. Y., Goldsmith, G. R., and Fisher, J. B.: Tropical

https://doi.org/10.5194/egusphere-2026-3927
Preprint. Discussion started: 23 July 2026


forests are approaching critical temperature thresholds, Nature, 621, 105-111, 10.1038/s41586-023-06391-z, 2023.

Dunn, R. J. H., Alexander, L. V., Donat, M. G., Zhang, X., Bador, M., Herold, N., and al., e.: Development of an updated global land in-situ-based dataset of temperature and precipitation extremes: HadEX3, JGR: Atmospheres, 125, e2019JD032263, 10.1029/2019JD032263., 2020.

Forkel, M., Carvalhais, N., Rödenbeck, C., Keeling, R., Heimann, M., Thonicke, K., Zaehle, S., and Reichstein, M.: Enhanced seasonal $CO_2$ exchange caused by amplified plant productivity in northern ecosystems, Science, 351, 696-699, 10.1126/science.aac4971, 2016.

Forzieri, G., Dakos, V., McDowell, N. G., Ramdane, A., and Cescatti, A.: Emerging signals of declining forest resilience under climate change, Nature, 608, 534-539, 10.1038/s41586-022-04959-9, 2022.

Graven, H., Keeling, R., Piper, S., Patra, P., Stephens, B., Wofsy, S., Welp, L., Sweeney, C., Tans, P., and Kelley, J.: Enhanced seasonal exchange of $CO_2$ by northern ecosystems since 1960, Science, 341, 1085-1089, 10.1126/science.1239207, 2013.

Grossiord, C., Buckley, T. N., Cernusak, L. A., Novick, K. A., Poulter, B., Siegwolf, R. T. W., Sperry, J. S., and McDowell, N. G.: Plant responses to rising vapor pressure deficit, New Phytol, 226, 1550-1566, 10.1111/nph.16485, 2020.

Haverd, V., Smith, B., Canadell, J. G., Cuntz, M., Mikaloff-Fletcher, S., Farquhar, G., Woodgate, W., Briggs, P. R., and Trudinger, C. M.: Higher than expected $CO_2$ fertilization inferred from leaf to global observations, Global Change Biology, 26, 2390-2402, 10.1111/gcb.14950, 2020.

Hubau, W., Lewis, S. L., Phillips, O. L., Affum-Baffoe, K., Beeckman, H., Cuní-Sanchez, A., Daniels, A. K., Ewango, C. E. N., Fauset, S., Mukinzi, J. M., Sheil, D., Sonké, B., Sullivan, M. J. P., Sunderland, T. C. H., Taedoumg, H., Thomas, S. C., White, L. J. T., Abernethy, K. A., Adu-Bredu, S., Amani, C. A., Baker, T. R., Banin, L. F., Baya, F., Begne, S. K., Bennett, A. C., Benedet, F., Bitariho, R., Bocko, Y. E., Boeckx, P., Boundja, P., Brienen, R. J. W., Brncic, T., Chezeaux, E., Chuyong, G. B., Clark, C. J., Collins, M., Comiskey, J. A., Coomes, D. A., Dargie, G. C., de Haulleville, T., Kamdem, M. N. D., Doucet, J.-L., Esquivel-Muelbert, A., Feldpausch, T. R., Fofanah, A., Foli, E. G., Gilpin, M., Gloor, E., Gonmadje, C., Gourlet-Fleury, S., Hall, J. S., Hamilton, A. C., Harris, D. J., Hart, T. B., Hockemba, M. B. N., Hladik, A., Ifo, S. A., Jeffery, K. J., Jucker, T., Yakusu, E. K., Kearsley, E., Kenfack, D., Koch, A., Leal, M. E., Levesley, A., Lindsell, J. A., Lisingo, J., Lopez-Gonzalez, G., Lovett, J. C., Makana, J.-R., Malhi, Y., Marshall, A. R., Martin, J., Martin, E. H., Mbayu, F. M., Medjibe, V. P., Mihindou, V., Mitchard, E. T. A., Moore, S., Munishi, P. K. T., Bengone, N. N., Ojo, L., Ondo,

https://doi.org/10.5194/egusphere-2026-3927
Preprint. Discussion started: 23 July 2026


F. E., Peh, K. S. H., Pickavance, G. C., Poulsen, A. D., Poulsen, J. R., Qie, L., Reitsma, J., Rovero, F., Swaine, M. D., Talbot, J., Taplin, J., Taylor, D. M., Thomas, D. W., Toirambe, B., Mukendi, J. T., Tuagben, D., Umunay, P. M., van der Heijden, G. M. F., Verbeeck, H., Vleminckx, J., Willcock, S., Wöll, H., Woods, J. T., and Zemagho, L.: Asynchronous carbon sink saturation in African and Amazonian tropical forests, Nature, 579, 80-87, 10.1038/s41586-020-2035-0, 2020.

Levin, I., Kromer, B., Schmidt, M., and Sartorius, H.: A novel approach for independent budgeting of fossil fuel $CO_2$ over Europe by 14CO2 observations, Geophysical Research Letters, 30, 10.1029/2003GL018477, 2003.

Liu, Y., Peñuelas, J., Cescatti, A., Zhang, Y., and Zhang, Z.: Atmospheric Dryness Dominates Afternoon Depression of Global Terrestrial Photosynthesis, Geophysical Research Letters, 51, e2024GL110954, 10.1029/2024GL110954, 2024a.

Liu, Z., Rogers, B. M., Keppel-Aleks, G., Helbig, M., Ballantyne, A. P., Kimball, J. S., Chatterjee, A., Foster, A., Kaushik, A., Virkkala, A.-M., Burrell, A. L., Schwalm, C., Sweeney, C., Schuur, E. A. G., Dean, J., Watts, J. D., Kim, J. E., Wang, J. A., Hu, L., Welp, L., Berner, L. T., Mauritz, M., Mack, M., Parazoo, N. C., Madani, N., Keeling, R., Commane, R., Goetz, S., Piao, S., Natali, S. M., Wang, W., Buermann, W., Walker, X., Lin, X., Wang, X., Jin, Y., Yu, K., and Zhang, Y.: Seasonal CO2 amplitude in northern high latitudes, Nature Reviews Earth & Environment, 5, 802-817, 10.1038/s43017-024-00600-7, 2024b.

Margalef-Marrase, J., Pérez-Navarro, M. Á., and Lloret, F.: Relationship between heatwave-induced forest die-off and climatic suitability in multiple tree species, Global Change Biology, 26, 3134-3146, 10.1111/gcb.15042, 2020.

Muggeo, V. M.: Estimating regression models with unknown break-points, Statistics in medicine, 22, 3055-3071, 10.1002/sim.1545, 2003.

Muggeo, V. M. R., Atkins, D. C., Gallop, R. J., and Dimidjian, S.: Segmented mixed models with random changepoints: a maximum likelihood approach with application to treatment for depression study, Statistical Modelling, 14, 293-313, 10.1177/1471082X13504721, 2014.

Nath, D., Nath, R., and Chen, W.: Faster dieback of rainforests altering tropical carbon sinks under climate change, npj Climate and Atmospheric Science, 7, 235, 10.1038/s41612-024-00793-0, 2024.

Pan, Y., Birdsey, R. A., Fang, J., Houghton, R., Kauppi, P. E., Kurz, W. A., Phillips, O. L., Shvidenko, A., Lewis, S. L., Canadell, J. G., Ciais, P., Jackson, R. B., Pacala, S. W., McGuire, A. D., Piao, S., Rautiainen, A., Sitch, S., and Hayes, D.: A large and persistent carbon sink in the world's forests, Science, 333, 988-993, 10.1126/science.1201609, 2011.

https://doi.org/10.5194/egusphere-2026-3927
Preprint. Discussion started: 23 July 2026


549 Rasmusson, E. M. and Wallace, J. M.: Meteorological aspects of the El niño/Southern
550 Oscillation, Science, 222, 1195-1202, 10.1126/science.222.4629.1195, 1983.
551 Rotty, R. M.: Estimates of seasonal variation in fossil fuel $CO_2$ emissions, Tellus B: Chemical
552 and Physical Meteorology, 39, 184-202, 10.3402/tellusb.v39i1-2.15336, 1987.
553 Ruehr, S., Keenan, T. F., Williams, C., Zhou, Y., Lu, X., Bastos, A., Canadell, J. G., Prentice, I.
554 C., Sitch, S., and Terrer, C.: Evidence and attribution of the enhanced land carbon sink, Nature
555 Reviews Earth & Environment, 4, 518-534, 10.1038/s43017-023-00456-3, 2023.
556 Slik, J. W. F.: El Niño droughts and their effects on tree species composition and diversity in
557 tropical rain forests, Oecologia, 141, 114-120, 10.1007/s00442-004-1635-y, 2004.
558 Slot, M. and Winter, K.: In situ temperature response of photosynthesis of 42 tree and liana
559 species in the canopy of two Panamanian lowland tropical forests with contrasting rainfall
560 regimes, New Phytologist, 214, 1103-1117, 10.1111/nph.14469, 2017.
561 Tang, W., Zhang, F., Stoy, P. C., Scott, R. L., Tang, A. C. I., and Fu, Z.: Contribution of Carbon
562 Dioxide Concentration to the Diurnal Variation in Land Surface Carbon Dioxide Uptake From
563 the Atmosphere, Plant, Cell & Environment, 48, 6722-6733, 10.1111/pce.15638, 2025.
564 Teskey, R., Wertin, T., Bauweraerts, I., Ameye, M., McGuire, M. A., and Steppe, K.: Responses
565 of tree species to heat waves and extreme heat events, Plant Cell Environ, 38, 1699-1712,
566 10.1111/pce.12417, 2015.
567 von Caemmerer, S.: Rubisco carboxylase/oxygenase: From the enzyme to the globe: A gas
568 exchange perspective, Journal of Plant Physiology, 252, 153240, 10.1016/j.jplph.2020.153240,
569 2020.
570 Wang, K., Yan, H., Guo, X., Lin, Q., Li, J., Peng, A., Fu, Y., Gong, Z., Yang, S., and Ding, Y.:
571 FERONIA orchestrates plasma membrane nanoclusters for plant thermotolerance, Science,
572 392, 885-890, 10.1126/science.aeb1752, 2026.
573 Zhang, M., Cheng, Y., Bao, Y., Zhao, C., Wang, G., Zhang, Y., Song, Z., Wu, Z., and Qiao, F.:
574 Seasonal to decadal spatiotemporal variations of the global ocean carbon sink, Global Change
575 Biology, 28, 1786-1797, 10.1111/gcb.16031, 2022.
576 Zhu, Z. C., Piao, S. L., Myneni, R. B., Huang, M. T., Zeng, Z. Z., Canadell, J. G., Ciais, P.,
577 Sitch, S., Friedlingstein, P., Arneth, A., Cao, C. X., Cheng, L., Kato, E., Koven, C., Li, Y., Lian,
578 X., Liu, Y. W., Liu, R. G., Mao, J. F., Pan, Y. Z., Peng, S. S., Penuelas, J., Poulter, B., Pugh, T.
579 A. M., Stocker, B. D., Viovy, N., Wang, X. H., Wang, Y. P., Xiao, Z. Q., Yang, H., Zaehle, S.,
580 and Zeng, N.: Greening of the Earth and its drivers, Nature Climate Change, 6, 791-+,
581 10.1038/Nclimate3004, 2016.
582